Advanced Materials Progress Report on

Bio-inspired Materials Chemistry**

By *Erik Dujardin* and *Stephen Mann**

Progress reports are a new type of article in Advanced Materials, dealing with the hottest current topics, and providing readers with a critically selected overview of important progress in these fields. It is not intended that the articles be comprehensive, but rather insightful, selective, critical, opinionated, and even visionary. We have approached scientists we believe are at the very forefront of these fields to contribute the articles, which will appear on an annual basis. The article below describes the latest advances in bio-inspired materials chemistry.

1. Introduction

With the notable exception of biomineralization,[1] biology and materials chemistry were until very recently hermetically separated research areas. In the past few years, however, a growing number of interdisciplinary research projects at the frontier between these two fields have emerged. Central to many of these developments is the notion of bio-inspiration, in which biological concepts, mechanisms, functions, and design features are abstracted as starting points on the road to new synthetic materials and devices with advanced structures and functions. In general, the aim is not to emulate a particular biological architecture or system but to use such knowledge as a source of guiding principles and ideas. The underlying philosophy is based therefore on what might be termed "soft interpretation", along with a large element of imagination!

Bio-inspired materials chemistry—also referred to as *biomimetic materials chemistry*[2]—is an important aspect of diverse fields, such as bioceramics, biosensing, biomedical engineering, bionanotechnology, and biologically driven materials self-assembly. More than any previous year, 2001 witnessed an increase in the number of new investigations at the interface between materials chemistry and biology, which we review in this article. The review is organized in four sections. In Section 2, we describe current strategies to develop biologically compatible solid surfaces as well as the use of biological systems to design smart inorganic interfaces. Section 3 focuses on current progress in the well-established field of bio-inorganic materials synthesis and biomineralization, and related areas such as sol–gel bio-encapsulation ("mineralized biology"), bioceramics, and bioglasses. Because self-assembly is a key driving force in the integration of biological and artificial materials, Section 4 discusses routes to self-organization and higher-order architectures with a particular emphasis on DNA-derived approaches using biomolecular linkers or inorganic nanoparticles. The last section highlights the importance of the nanoscale in bio-inspired materials chemistry, and reviews recent advances in the synthesis and application of bio-inorganic nanoparticles.

2. Bio-smart Interfaces

The remarkable ability of biological organisms to recognize, sort, and process diverse and complex sources of information continues to inspire novel approaches to the fabrication of smart inorganic-based surfaces and interfaces. A striking increase in papers focused on the nanostructuring or precise binding of biological molecules to technologically relevant solid interfaces was apparent throughout 2001.[3–12] By combining known technologies such as lithography or surface probe microscopies[13,14] and complex functions or recognition abilities of biological systems,[15,16] micro- and nanometer-scale architectures that integrate features such as anisotropy,[3,4] specific binding,[5–8] or motion[9–12] have been designed for potential applications in active nanodevices[17–22] dealing with electronic information and mechanical tasks, pre-encoded surface coatings for clinical testing and screening, structure–function elucidation, and new interface probes.

Surfaces as diverse as gold, silica, and graphite have been functionalized with proteins or oligonucleotides by non-specific adsorption or specific interfacial interactions involving covalent or electrostatic bonding to produce inorganic substrates with recognition capabilities towards natural substrates

[*] Prof. S. Mann, Dr. E. Dujardin[+]
School of Chemistry, University of Bristol
Cantock's Close, Bristol BS8 1TS (UK)
E-mail: s.mann@bristol.ac.uk

[+] Present address: CEA/DRECAM/SCM, bát. 125, CEA/Saclay, F-91191 Gif-sur-Yvette, France.

[**] E. D. acknowledges the European Union for a Marie Curie Individual Fellowship (HPMF-CT-1999-00254).

  0935-9648/02/1106-0775 $ 17.50+.50/0

ADVANCED MATERIALS

and related biomolecules. For example, the binding of bovine serum albumins (BSA) on glass substrates favored the ordering of a liquid crystalline layer of 4-cyano-4M′-pentylbiphenyl placed on top of the BSA layer.[6] By derivatizing the lysine moieties of BSA, various antibody receptors could be attached to the albumin, which then became a versatile linker between antibodies in solution and the solid surface. In the absence of antibodies, the rubbed BSA surface induced a highly ordered nematic phase of the 4-cyano-4M′-pentylbiphenyl layer but when a complementary antibody was introduced the uniform alignment was completely disrupted allowing optical detection of the antigen–antibody recognition event when the solid substrate was placed between crossed polarizers.[6] No such disruption occurred in the presence of non-specific antibodies. Similar studies with human BSA used silica substrates that were biologically "primed" prior to protein immobilization.[7] For this, a unilamellar bilayer of phospholipid was supported on silica beads to produce substrates with membrane-mimetic properties. When a Ca^{2+} ATPase was inserted in a second bilayer around the coated beads, the enzymatic activity was fully retained, whereas a 90 % loss in function was observed for non-coated beads.

The integration of biological systems with standard microelectronics opens new perspectives for developing novel biosensors or neuronal memory devices and prosthetics. Several conditions must be fulfilled: i) Recognition between the sensor surface and analyte must be selective and reversible. ii) Sensitivity of the detection method or signal processing must be high enough to record single events. iii) High levels of compatibility between the artificial device and biological interface must be ensured. Selective recognition can be achieved by a variety of approaches.[15,16] For example, immobilization of the lactose (*lac*) repressor protein of *Escherichia coli* on a gold surface makes it possible to selectively recognize linear plasmid DNA containing the full sequence of the *lac* operator.[17] As molecular promoters of the *lac* repressor protein, such as galactose derivatives, prevent binding to the operator DNA, capacitive detection of the promoters could be performed over a concentration range of 1 nM to 10 mM. For larger structures such as living cells, recognition mechanisms based on the frequency variation of quartz crystal microbalances (QCMs) have been used for selective detection (Fig. 1).[18] The QCM was coated with polymerizing polyurethane onto which the micro-organisms were gently pressed. The polymer imprint was not only geometrically defined, which gave rise to cell size selectivity, but also chemically and topologically specific, and hence highly selective to species of a given cell family.

The high sensitivity of natural sensory systems is often based on the use of membrane-bound receptors such as ion

Stephen Mann obtained a B.Sc. degree in Chemistry from UMIST after which he carried out his Ph.D. with Prof. R. J. P. Williams at the University of Oxford. After a Junior Research Fellowship at Keble College, Oxford, he was appointed to an academic position at the University of Bath where he stayed from 1984 until 1998 when he moved to the University of Bristol as Professor of Chemistry and Director of the Centre for Organised Matter Chemistry. Research by Stephen Mann and colleagues has led to an increased understanding of biomineralization and the parallel development of new biomimetic approaches in materials synthesis. Prof. Mann's work has been focused particularly on the nanoworld of rusty proteins and magnetic bacteria, as well as the beautiful complex forms of microscopic skeletons and shells. At the moment, he is particularly excited about the use of complex fluids to facilitate emergent behavior—such as biomimetic form and hierarchy—during the synthesis of inorganic-based materials. He has obtained awards from the Royal Society of Chemistry (Corday-Morgan Medal in 1993 and RSC Interdisciplinary Award in 1999), and is a recipient of the Max Planck Research Prize for International Cooperation, awarded in 1998.

Erik Dujardin received his R&D engineer diploma from the Ecole Supérieure de Physique et Chimie Industrielles (ESPCI, Paris, France), where he was trained in both physics and chemistry. His main research interests are in the design and characterization of new materials with specific physical properties as well as the study of materials properties at the nanoscale level. As an undergraduate, he studied organic photochromic materials with Prof. J.-M. Lehn (Collège de France, Paris) before joining Prof. M. Verdaguer's group (Univ. P. and M. Curie, Paris) for one year, where he worked on molecular magnetic materials. He received his Ph.D. from the University of P. and M. Curie in Paris in 1999. During his doctoral studies with Prof. T. W. Ebbesen at the NEC Research Institute (Princeton, NJ), his interests focused on the size effects on mechanical, electronic and interfacial properties of curved and flat graphitic materials. In 2000 and 2001, he worked as a Marie Curie post-doctoral fellow in Prof. S. Mann's group where he was involved in various projects in biomimetic nanomaterial chemistry ranging from nanoparticle synthesis to higher order organization of metallic nanowires. His second and current post-doctoral position, with Dr. J.-P. Bourgoin in the Molecular Electronic Laboratory of the French Atomic Energy Commission (CEA, Saclay, France), is dedicated to measuring electronic properties of individual molecules at the silicium interface.

  0935-9648/02/1106-0776 $ 17.50+.50/0

ADVANCED MATERIALS

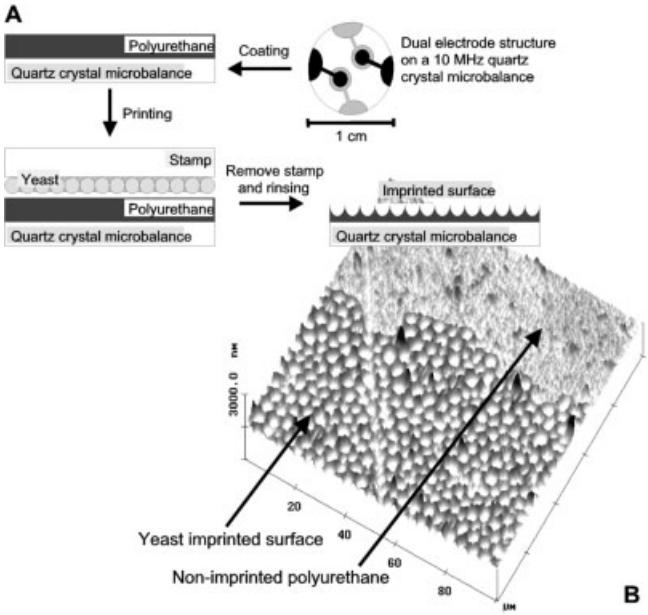

Fig. 1. Selective detection of yeast cells by surface imprinting. A) A polyurethane-coated QCM is printed overnight with a stamp of *S. cerevisiae* cells, which is subsequently removed and rinsed with hot water. B) Tapping mode AFM image of the sensor layer showing imprinted and non-imprinted polyurethane areas. Reproduced with permission from [18].

channels, and bio-inspired systems using stochastic sensors are emerging in single-molecule detection technology.[19] The basic strategy involved the incorporation of a single ion-conducting channel, such as the α-haemolysin (αHL) complex, within a planar lipid bilayer. Modification of the interior channel of αHL with histidine ligands (for divalent metal ions), single stranded oligonucleotides (for DNA duplex formation) or β-cyclodextrin (for small hydrophobic organic molecules) gave rise to single binding events that influence the ionic current recorded across the membrane pores. Measuring the intra- and extracellular potential of neurons is another highly sensitive method.[13] For example, single intracellular voltage pulses were detected or stimulated automatically on a single neuron located at the surface of a silicon field-effect transistor.[20]

Biocompatibility in sensors or devices technology often relies on attaching surface recognition moieties. For instance, close interfacing between CdS nanoparticles and human neurons was achieved by attaching to the quantum dots a peptide sequence known to bind specific cell surface receptors (integrins) (Fig. 2).[21] The main asset of this approach lies in the short distance between the semiconductor particle and neuronal cell, which could facilitate electron transfer in neuronal prosthetic devices. In another study, coatings of collagen I were shown to facilitate the adhesion of primary hepatocytes cells to porous silicon.[22] The hepatocytes remained viable and maintained normal liver-specific functions for several days.

A significant development in the fabrication of bio-smart interfaces involves the introduction of receptors that can act as mechanical transducers or exhibit directional surface motion. For example, biomolecular motors, such as F_1-ATPase[9]

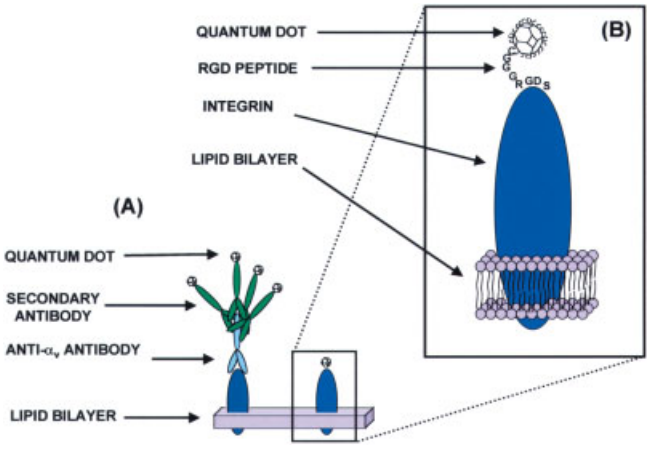

Fig. 2. Biocompatible linking of CdS nanoparticles to nerve cells. A) coupling through amine bonds to secondary antibodies that are linked to a primary antibody embedded in the lipid membrane, and B) coupling to integrin receptors via RGD peptide recognition sequence attached to the nanoparticle surface. Reproduced with permission from [21].

or kinesin,[10–12] have recently been tethered to plain or nanopatterned surfaces with a view to combine self-propelling enzymes with nano-electro-mechanical systems (NEMSs). F_1-ATPase is a 10 nm rotary molecular motor that spins at ca. 17 rps as it synthesizes adenosine triphosphate (ATP) to produce 80 pN nm of work. Arrays of 60 to 600 nm nickel dots were deposited on a silicon wafer using conventional lithographic techniques and up to three F_1-ATPase molecules per dot were coupled through specially engineered histidine moieties.[9] Similarly, tubulin/kinesin conjugates can be envisioned as elementary units of a "tinker toy" approach to surfaces patterned with nanoscale motors.[10,11] Kinesin is an ATP-powered molecular motor that steps along the grooves on the surface of the tubulin microtubules. For each ATP hydrolyzed, the kinesin moves by an 8 nm step from the so-called minus end to the plus end of the microtubules. Limberis et al. attached microtubules on silica surfaces via an α-tubulin antibody, which binds to the minus end of the microtubule only.[10] The other side of the antibody was bound to a surfactant that ensured adsorption onto the substrate. By this process, the microtubules were hampered at their minus end but free to align under flow shearing to create oriented tracks along which kinesin could wander in a predetermined direction. In contrast, Hess et al. adsorbed kinesin molecules at the bottom of grooves patterned in a resin surface.[11] When microtubules were added on top of the kinesin, they moved along the grooves powered by the kinesin motors underneath and guided by the surface topology. If the microtubules were covered with biotin so that beads covered with streptavidin could be positioned in the immediate pathway of the guided microtubule, the moving microtubule captured the beads and carried them along before releasing them further down the track. Moreover, pulses in the concentration of free ATP could be used to control the amount of energy injected into the motor system and hence the motion of the microtubules along the kinesin tracks.

  0935-9648/02/1106-0777 $ 17.50+.50/0

It is clear from the above examples that tools for engineering bio-smart interfaces using functionalized inorganic substrates are becoming ever more available and that understanding and manipulation of surface interactions is developing rapidly. Two major potential outcomes of this progress can be underlined already. Firstly, complex functions, which have naturally evolved in the biological world, will be used routinely in the future to confer advanced capabilities to man-made materials and architectures. Secondly, new insights into the preparation of biocompatible materials and interfaces will accelerate the creation of probes, sensors, and implants for use in bionic systems of matter. These developments also depend on advances in our knowledge of native biological materials, such as biominerals, which we review in the next section.

3. Bio-inorganic Materials

In recent years, several areas of materials research have been inspired by the study of biominerals.[1] Here we discuss three themes. Firstly, understanding the growth and form of biologically relevant minerals, such as calcium phosphate, calcium carbonate and silica, continues to be aided by model studies involving the deposition of these solids in the presence of organic molecules and surfaces (Sec. 3.1). Secondly, the laboratory mineralization of biological structures and systems to produce inorganic materials with incarcerated components such as viruses and cells is a central thrust of biomimetic materials synthesis (Sec. 3.2). Thirdly, the mechanical design of many biominerals combines antagonistic properties that are difficult to obtain in artificial ceramics—bone, for example, consists of a protein/calcium phosphate nanocomposite that has high fracture toughness and strength yet is efficient at stress damping—so the preparation and processing of biomimetic materials for use in dental or orthopedic applications is of major concern (Sec. 3.3).

3.1. Biomineralization

Biominerals have fascinated materials scientists for a long time, and recent studies, such as on the skeletal photoreceptor system of the brittlestar *Ophiocoma wendtii*, continue to reveal remarkable multi-functional and integrative properties (Fig. 3).[23] *O. wendtii* is a highly photoresponsive species that changes color from day to night and escapes to dark crevices whenever it detects the shadow of a potential predator. However, no eyes have been documented in studies on brittlestars. The new analysis of the complex calcitic skeleton showed the presence of a regular array of spherical microstructures with characteristic double-lens shapes. Photolithographic experiments proved that the microlenses guide and focus visible light onto nerve bundles, which are thought to be primary photoreceptors. The lens array is designed to minimize spherical aberration and birefringence by profiling the top and bottom faces, and orientating the single crystal of calcite, respectively. Furthermore, the array detects the light from a specific direction with an angular selectivity of 10° and chromophores optimize the system by regulating the illumination dose reaching the receptors.

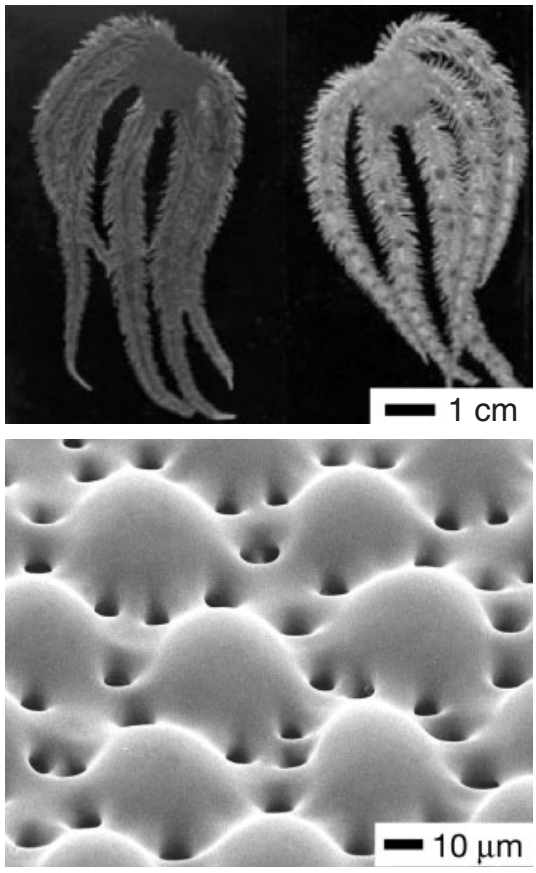

Fig. 3. a) Light sensitive brittlestar, *O. wendtii*, in daylight (left) and at night (right). b) SEM image of the peripheral layer of a dorsal arm plate showing the spherical microlens array. Reproduced with permission from *Nature* [23]. Copyright 2001 Macmillan Publishing Ltd.

Biominerals are usually synthesized at the surface of organic templates such as macromolecular frameworks, lipid membranes or cell walls. In order to achieve these biomineralization processes, specific interactions, selective organic moieties and biocompatible minerals have evolved. A recent AFM study has shown the complexity underlying cell/mineral interactions in the case of the bacterium, *Shewanella oneidensis*, and iron oxide mineral, goethite (α-FeOOH).[24] *S. oneidensis* is a dissimilatory metal-reducing bacterium, which oxidizes organic matter in oxygen-deficient environments by reductively dissolving iron(III)-rich minerals. By careful grafting of fully functional cells onto cantilever probes of a force microscope, Lower et al. measured the sub-nanonewton forces between the complex biomolecular network on the surface of the bacteria and well-defined goethite crystal faces. The adhesion energy of *S. oneidensis* to goethite was 2 to 5 times greater in anaerobic conditions than in the presence of oxygen. In contrast, it remained constant when non-viable bacteria or iron-

0935-9648/02/1106-0778 $ 17.50+.50/0

ADVANCED MATERIALS

free oxyhydroxydes, such as diaspore (α-AlOOH), were substituted in the experiment. In addition, sawtooth-like discontinuities in the force curves suggested that a 150 kD iron reductase present in the outer membrane active was responsible for recognition of the mineral by the cell.

The general importance of proteins and peptides in controlling the nucleation and/or growth stages of mineralization has continued to be demonstrated by many in-vitro studies of calcium carbonate crystallization. For example, chiral crystals of calcite were formed in the presence of pure D- or L-aspartic acid due to preferential binding of amino acid enantiomers to the surface steps that offer the best geometrical and chemical match.[25] Homo- or heteropolymers of amino acids also have a marked influence on calcium carbonate crystallization.[26] Elongated needles of aragonite were produced in the presence of poly(Asp-Leu), whereas crystallization was inhibited with poly(Glu-Leu). Addition of proteins extracted from the sea urchin *Evechinus chloroticus* to a supersaturated solution of calcium carbonate produced porous inorganic morphologies that were reminiscent of the natural sea urchin skeleton.[27]

The influence of polyacrylic acid on $CaCO_3$ crystallization has been reported by Naka and Chujo.[26] They showed that the precipitation of one of the three polymorphs of $CaCO_3$ can be induced at low temperature (30 °C) by triggering the polymerization of acrylic acid after different aging times in a calcium carbonate supersaturated solution. Aragonite needles were formed after 1 min, spherical vaterite after 3 min, and rhombohedral calcite after 20 min. The cooperative effect of aqueous solutions of poly(acrylic acid) and insoluble polysaccharide substrates (cellulose, chitin, chitosan) has also been studied.[28] When all proton-donor or -acceptor groups of the polysaccharides are protected, no precipitation occurs. In the presence of NH and/or OH groups on the solid surface, but without the polymer solution, a polycrystalline calcite film was formed. With the polyacrylic acid, the crystal phase was calcite in the case of cellulose and chitin, but vaterite in the presence of chitosan. The results were explained on the basis that surface groups of the substrate or functional groups on the adsorbed polymers, or both, interact with calcium ions to increase the local concentration sufficiently to kinetically induce the precipitation of thermodynamically unstable polymorphs such as vaterite.

A variety of synthetic substrates and their effect on the controlled morphogenesis of calcium carbonate have been reviewed recently.[26] In particular, carboxylate-terminated poly(amidoamine) (PAMAM) dendrimers are active as crystal habit modifiers. The carboxylate-rich surface of PAMAM sequesters calcium ions and thus stabilizes the vaterite phase. Changing the generation number of the dendrimer, modifies the surface charge and topology of the organic macromolecule, which in turn influences the size distribution and shape of the vaterite particles. Even larger objects with carboxylic acid moieties can be used to generate vaterite architectures with unusual morphologies. For example, vaterite crystals were nucleated around gold nanoparticles capped with surface-coupled mercaptobenzoic acid moieties.[29] Interestingly, when Mg^{2+} was added at a 1:1 molar ratio with Ca^{2+}, 150 nm diameter needles having a gold core and an aragonite shell were formed.

Compared with calcium carbonate, fewer studies were reported in 2001 on the effect of organic macromolecules on calcium phosphate crystallization. One remarkable system, however, concerned the study of fluoroapatite–gelatin composites as a model system for building nano- and meso-structured materials exhibiting some of the characteristics of tooth enamel.[30] Starting from an elongated hexagonal seed, the fluoroapatite crystals grow within the polypeptide gel by a complex process in which needle-shaped prisms were added at the ends of the seed to produce an equatorially notched macroscopic spheroid (Fig. 4). During growth, successive generations were arranged so that the angle between the long

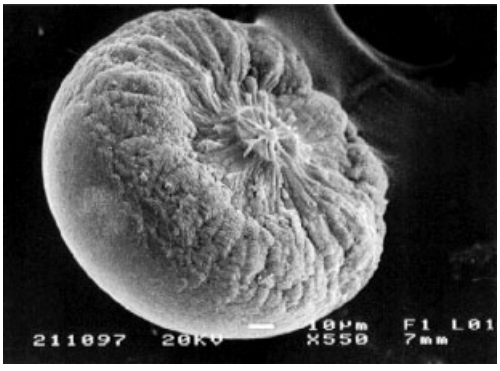

Fig. 4. SEM image showing half of an equatorially notched fluoroapatite-gelatine spheroid. Scale bar is 10 μm. Reproduced with permission from *Chemistry of Materials* [30]. Copyright 2001 American Chemical Society.

axes of the mother and daughter crystals was close to 45° and the scaling down factor about 0.7. The fractal structure resulting from these simple criteria produced surface crystals having a 50 nm average diameter, which is similar to the dimensions of enamel crystals. Moreover, in a second mineralization stage, the notched sphere served as a template for the formation of a shell consisting of highly anisotropic fluoroapatite particles that were closely packed radially in a striking resemblance to enamel structure.

Whereas enamel morphology is mainly dictated by proteins such as hydrophobic amelogenins and acidic enamelins, the extended polymeric matrix of collagen directs the hydroxyapatite (HAP) mineral in bones. In-vitro studies reported morphological alterations of HAP crystals by polypeptides present in dissolution experiments.[31] Compared to dissolution in pure water, dissolution and growth behavior of the crystal surfaces were altered in the presence of poly(sodium)aspartate, which lowered the interfacial energy. Furthermore, bovine serum albumin interacted with the calcium phosphate crystals by two mechanisms involving anionic aspartate moieties, which stabilized the calcium-rich faces, and cationic lysine groups that selectively bound to the phosphate ions.

  0935-9648/02/1106-0779 $ 17.50+.50/0

3.2. Mineralized Biology

One of the many remarkable features of bone is the integration of living cells within the mineralized collagen matrix. Not only are the cells biochemically active but they also communicate to each other as well as to cells outside the tissue so that the mineral becomes an integrated system capable of adaptation. The synthesis and processing of analogous artificial systems is far from being realized and represents a major challenge and paradigm shift in biomimetic materials chemistry.

Currently, there are many studies describing the encapsulation of biomolecules within inert inorganic matrices such as silica. In many cases, the biomolecules are used as functional units within a porous medium. For example, chlorophyll *a* and *b* pigments have been chemically grafted post-synthetically onto the internal surfaces of a mesoporous silica modified with α,ω-diols.[32] Energy transfer from chlorophyll *a* to chlorophyll *b* occurred even at low surface coverage with high efficiency (70 %), comparable to that obtained in other confined environments, such as micellar solutions (80 %), and much higher than in solution (< 50 %). The close proximity of the pigments on the silica surface probably accounts for the high efficiency of the Förster-type donor–acceptor interaction. Alternatively, the incarcerated biomolecules are used as shape- and size-selective porogens that are removed thermally after mineralization. For example, casting concentrated solutions of cyclodextrins (CDs) with silica resulted in hybrid composites that, when heated to high temperatures, produced an inorganic replica with short range ordered mesopores, 1.5 to 2 nm in size.[33] The ordering arose from maximization of overlap between the hydrophobic domains (inner side) and between hydrophilic domains (outer surface) of adjacent CD molecules that result in stacked filaments, which are subsequently replicated into a worm-like network of pores after calcination. Increasing the solubility of the CD molecules decreased the level of order, whereas more ordered mesopores were produced if the inner cavity was rendered more hydrophobic by including a hydrophobic guest.

In contrast with studies on molecular entrapment, there are few investigations on the incarceration within inorganic matrices of proteins or whole cells; however, the field appears to be developing. One of the major issues is to immobilize these relatively large biological components in the solid matrix without loss of structural integrity and functionality, and in this regard, the soft conditions of sol–gel processes appear to be very promising.[34] For example, modified strains of *E. coli* were successfully encapsulated in silica and their functional integrity tested within the solid substrate.[35,36] It was shown that an alkoxide route to silica (typically acidic hydrolysis of tetramethoxysilane) was not detrimental to the bacterial cells provided that the concentrations of the silica precursors and methanol by-product were kept below 0.01 M at any time.[35,36] Immediately after encapsulation, the *p*-nitrophenol production by the intracellular β-galactosidase enzymatic hydrolysis of 4-nitrophenyl-β-D-galactopyranoside (*p*-NPG) was comparable to the level observed in freely suspended cells.[35] Replacing the alkoxide reactant with an aqueous mixture of colloidal silica particles and sodium silicate that were subsequently condensed by acidification in a buffered medium proved to be less damaging to the cell membrane.[35] Similar studies using silica-entrapped luminous recombinant strains of *E. coli* showed full luciferase activity as evidenced by luminescence measurements on the solid gel.[36] Together, these studies highlight two crucial points: i) bacteria cells can remain structurally intact and functional after encapsulation in silica, and ii) the silica matrix is sufficiently porous and the encapsulated cell membranes permeable enough to allow enzymatic substrates to diffuse from the external aqueous solution to the cell membrane followed by transfer into the intracellular space.

Other studies have cast intact biostructures in silica. For example, highly ordered silica replicas were produced by surfactant-assisted mineralization of wood tissues.[37] Poplar and pine wood pieces were soaked in pre-hydrolyzed water/ethanol solutions of tetraethoxysilane in the presence of cetyltrimethylammonium bromide (CTAB). CTAB is known to be a porogen molecule in MCM-type mesoporous silica and to favor adsorption of incipient silica precursor species to solid surfaces. Moreover, interactions between the polar groups of cellulose and lignin with the silicate precursors appeared to be responsible for a high level of condensation within the wood tissue rather than on the outer surface. Consequently, calcination of the composite produced a mesoporous silica monolith that was a replica of the wood cellular structures on length scales from the largest fibrous features to sub-micrometer striations. A similar approach was investigated using liquid crystalline gels of the rod-like tobacco mosaic virus (TMV) to prepare ordered mesoporous silica.[38] Controlled hydrolysis and condensation of mixtures of tetraethoxysilane and aminopropyltriethoxysilane within the interstitial spaces of the TMV nematic liquid crystal produced highly-ordered silica–TMV hybrid mesostructures, as illustrated in Figure 5. The TMV particles were incarcerated within the silica matrix and could be removed by calcination to produce replicas with hexagonally ordered (a=20 nm) cylindrical pores, 11 nm in diameter.

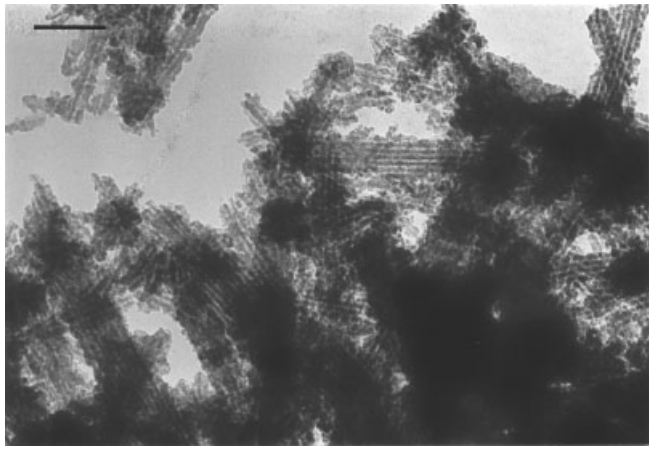

Fig. 5. TEM image of ordered TMV-silica mesostructures. Scale bar is 200 nm. Reproduced with permission from [38].

0935-9648/02/1106-0780 $ 17.50+.50/0

ADVANCED MATERIALS

3.3. Bioceramics and Bioglasses

While a microscopic understanding of bone mechanical behavior is still incomplete, the need for implants and bioactive fillers has prompted different strategies for combining the biocompatibility of hydroxyapaptite (HAP) with the mechanical robustness of other materials. Ceramic composites and bioglasses continue to be the two principal approaches. In general, bioceramics are produced by mixing calcium phosphates with another ceramic, such as zirconia, that is mechanically strong and biologically inert.[39,40] Processing techniques and nanostructure control remain crucial issues. In particular, HAP is decomposed at high temperatures in the presence of ZrO_2 by a reaction involving water diffusion. To circumvent this, a fast plasma sintering technique was used to fully densify the composites at low temperatures while avoiding water diffusion and associated degradation.[39] Alternatively, sol–gel synthesis was employed to synthesize stable, homogeneous, and well-defined HAP nanoparticles, which were easy to sinter at lower temperatures.[40] The nanoparticles were combined with a dilute yttria-stabilized zirconia sol to produce a uniform composite with improved fracture toughness of 2.0 MPa $m^{1/2}$, instead of 1.3 MPa $m^{1/2}$ for the pure nanostructured HAP (comparable values for bone are 2–12 MPa $m^{1/2}$).

Bioglasses embody a range of materials containing silica, sodium silicate, calcium, and phosphate, which form strong bonds with bone tissue, induce nucleation of HAP on their surface, and are easily colonized by osteoblasts. Mechanistic studies on the biomineralization of such glass surfaces by HAP have shown that calcium need not be present in the glass to form an amorphous calcium phosphate (ACP) coating.[41] When pure silica was immersed in a simulated body fluid, electrostatic interactions between surface silicate and calcium ions in the solution produced a slightly positively charged surface that induced phosphate adsorption and the subsequent nucleation of ACP. The growth of fluoroapatite on glass ceramics has also been reported.[42] By using an annealing temperature of 1200 °C, needle-like crystals with a 15:1 aspect ratio similar to enamel crystals were observed, which could be subsequently oriented within the ceramic matrix by extrusion processing.

The efficiency and extent of biomineralization of bioglasses are highly dependent on the meso- and macroporosity of the inorganic material. Macroporosity is essential for vascularization and tissue growth, which are key requirements if the implant is to be biologically integrated. Biomineralization of both mesoporous and macroporous glasses have been reported with encouraging results.[43,44] For example, Figure 6 shows a 3D ordered macroporous bioactive glass, which was exposed to simulated body fluid for three hours.[43] Small spheres of amorphous calcium phosphate completely covered the wall surfaces such that the glass template was buried under several micrometers of HAP within a few days. The silica–calcium oxide framework dissolved away as the HAP grew, with only 25 wt.-% of the initial bioglass left after seven days. This could be a major asset for some implant applications because new bone tissue would replace the bioglass filler with time. Similar studies have investigated the surface deposition of HAP on mesoporous silica.[44] The results indicated that the mesoporous structure had little effect on the growth and morphology of the HAP crystals.

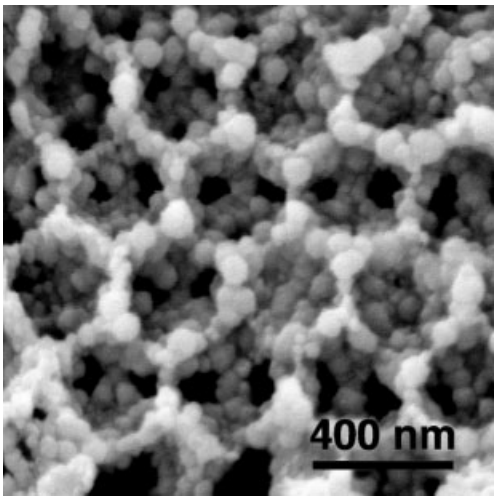

Fig. 6. SEM image of a 3D ordered macroporous bioglass structure after immersion in simulated body fluid for 3 h showing extensive overgrowth of amorphous calcium phosphate on the pore walls. Reproduced with permission from *Chemistry of Materials* [43]. Copyright 2001 American Chemical Society.

A significant breakthrough in the field of bioceramic and bioglasses would be the routine preparation of hybrid materials with multiple functionality. As a first step towards this goal, a recent study used a self-assembled surfactant architecture that was designed specifically to control the nucleation and growth of HAP, and provide potential recognition sites for cell adhesion.[45] The molecule consisted of a C_{16} alkyl chain to favor micelle formation, and a polar headgroup that was subdivided into blocks of different functional moieties. A block of four consecutive cysteine amino acids was chosen to promote robustness by intermolecular disulfide cross-linking, and a phosphoserine was inserted to form a highly phosphorylated interface, which promoted HAP nucleation at the surface of the micelle. In addition, the amphiphile was terminated with the amino acid sequence Arg-Gly-Asp (RGD), which plays an important role in cell adhesion. Although highly soluble at high pH, the micelles gelled at pH 4 into a network of nanofilaments that were 7.6 nm in diameter. At high surfactant concentrations, β sheet and α helical secondary structures were observed. When exposed to supersaturated calcium phosphate solutions, oriented platelets of HAP spontaneously coated the filaments.

The above examples show that directed nucleation and crystal growth, as well as template replication are important aspects that need to be considered in the preparation of advanced bioceramics and bioglasses. A future goal would involve the self-assembly of complex hybrid systems across a range of length scales. Such processes are used throughout biology, and are of major interest in the field of soft matter organization, as described in the next section.

  0935-9648/02/1106-0781 $ 17.50+.50/0

4. Self-Assembly and Higher Order Organization

The self-assembly of molecular building blocks into large architectures is a central feature in the chemistry of life. It has become a pivotal research theme for supramolecular chemists and many current nanotechnologies are based on self-organized systems. The main types of amphiphilic molecules used are surfactants, lipids, block copolymers, polysaccharides, and DNA. Several examples are given below.

4.1. Surfactants, Lipids, and Peptides

The efficiency of self-assembly of amphiphilic molecules at the colloidal level is striking. For example, colloidal particles resembling virus capsids were recently prepared from dilute salt-free mixtures of simple anionic ($CH_3(CH_2)_{12}CO_2H$) and cationic (cetyltrimethylammonium hydroxide) surfactant vesicles that contained a molar excess of the fatty acid.[46] Cooling the solutions below the chain melting temperature gave a colloidal solution of micrometer-sized hollow icosahedra (Fig. 7). The walls were composed of a bilayer of randomly distributed ion pairs except at the vertices, where the walls were enriched in fatty acid molecules. The excess negative charge prevents closure such that the vertices remain open to produce a porous hollow shell. Other studies have used mixtures of phospholipids to self-assemble twisted ribbons and nanotubules.[47] Nanotubules were obtained by slowly cooling an equimolar dispersion of 1,2-bis(tricosa-10,12-diynoyl)-*sn*-glycero-3-phosphocholine ($DC_{8,9}PC$) and 1,2-bis(dinonanoyl)-*sn*-glycero-3-phosphocholine (DNPC) from 60 °C to 4 °C. Typically, the nanotubules were 50 nm in diameter and up to several micrometers in length. Circular dichroism measurements indicated a chiral packing of the lipids in the tubule wall that was influenced by increasing the temperature, which produced a morphological transition from the twisted ribbon to the helical microtubule form.

Besides hydrophobic interactions, hydrogen bonding is a common driving force for self-assembly. For this reason, many peptides have proved to be highly versatile building blocks for preparing higher-order architectures with flat or tubular morphologies.[48–51] In particular, cyclic peptides have been self-assembled into short cylinders,[48] long nanotubes[49,50] or uniaxial crystalline materials,[49] and β-sheet peptides into "rigid-rod" β-barrels.[51] The synthesis, physical chemistry, and potential applications of such self-assembled organic nanotubes have been extensively reviewed.[50] As well as models of biological channels, these hollow tubular architectures could serve as macromolecular scaffolding or packaging analogous to natural microtubules and viral coat proteins.[52]

4.2. DNA

Another archetypal building block that employs hydrogen bond-based self-assembly is DNA. Whereas biological interactions involving DNA are mainly restricted to two DNA strands or one strand and a protein, materials chemists are developing new self-assembled objects, in which DNA is coupled, for example, to amphiphiles,[53] polymers,[54,55] organometallic complexes,[56,57] metallic ions,[58] or proteins (biotin).[59–62] The motivation to use DNA derives from the unusual combination of high recognition, selectivity, and polyanionic character. Moreover, DNA molecules can be readily conjugated and assembled into nanostructured materials by three strategies involving i) electrostatic interactions with the polyphosphate backbone, ii) covalent functionalization of either the 3′ or 5′ end of the oligonucleotide strand, or iii) covalent or electrostatic attachment to inorganic nanoparticles.

4.2.1. Charge Matching Assembly

Conjugation of DNA via charge interactions involving the phosphodiester groups can be applied to many cationic species. In particular, complexation of double stranded DNA with cationic surfactants has been widely explored as a means to extract, concentrate, and count DNA in cell transfection or gene therapy studies. Such interactions are also of interest in materials science; for example, free standing or surface-supported thin films of DNA–surfactant complexes have been prepared by slow evaporation.[53] Circular dichroism, thermogravimetry analysis, and X-ray diffraction showed that the DNA remains intact and is preferentially oriented within a lamellar

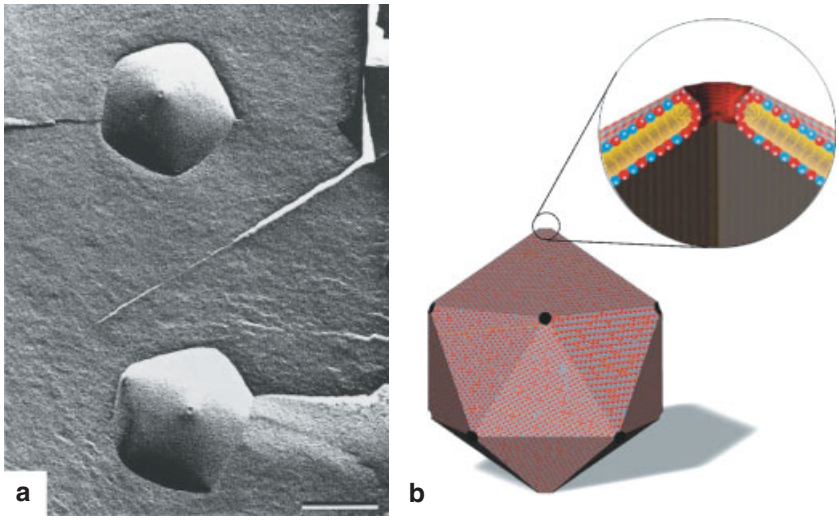

Fig. 7. a) Cryo-fracture TEM image of two adjacent surfactant icosahedral vesicles. The pentagonal symmetry around the porous vertices is clearly seen. Scale bar is 250 nm. b) Schematic representation of cationic/anionic aggregate structure. Flat faces, with a typical area of 0.3 μm^2, are made of about 10^6 ion pairs. The aggregates are stabilized by the 15 nm diameter pores produced by about 200 molecules. The regular icosahedron is the structure that best minimizes the bending energy of the rigid bilayers. Reproduced with permission from *Nature* [46]. Copyright 2001 Macmillan Publishing Ltd.

0935-9648/02/1106-0782 $ 17.50+.50/0

ADVANCED MATERIALS

surfactant mesophase. Moreover, the anisotropically ordered material induced the alignment of functional dye molecules that interact specifically with DNA. In another study, the polyanionic behavior of DNA was used to template the photocatalytic polymerization of long polyaniline chains.[54,55] In this system, the polyphosphate backbone was used to bind the photoactivated catalyst $[Ru(bpy)_3]^{2+}$ (bpy=2,2′-bipyridine) and lower the local pH so that the *N*-phenyl-*p*-phenylenediamine monomer becomes protonated and also bound to the DNA. The proximity of the electron donor and monomer obtained by co-assembly on the DNA template resulted in an increase in the efficiency of the photochemical reaction and formation of longer polymer chains. Furthermore, the DNA–polyaniline material obtained was successfully integrated into an organic light-emitting diode.

A similar templating approach was used to organize metallic nanoparticles into linear chains along DNA strands.[58] Calf thymus DNA was ion-exchanged with platinum(II) complexes prior to in-situ reduction to platinum(0) with borohydride salts. UV-vis spectrophotometry suggested that chlorine ligands in the original complexes were replaced by electron pairs from the N7 atoms of purine nucleotides (guanine or adenosine). After reduction, necklaces of metallic Pt nanoparticles with an average diameter of 1 nm could be observed by electron microscopy. In other studies, electrostatic interactions between DNA phosphate groups and preformed positively charged gold particles induced the alignment of nanoparticles along the DNA strands.[59]

4.2.2. Assembly via Covalent Functionalization

Covalent functionalization of one or both ends of the oligonucleotide strands of DNA for use in higher-order materials assembly is an exciting new area of research with much potential. For example, a whole new class of self-assembled architectures can be envisioned based on the covalent coupling of protein-binding molecules, such as biotin, at the end of a single oligonucleotide strand. In this case, the combination of DNA duplexation and biotin-streptavidin (STV) complexation provides a highly versatile means of directing the self-assembly of multi-component nanostructures. When the only available building blocks are a bis-biotinylated double stranded (ds) DNA and free strepavidin, Niemeyer et al. have shown that circular bis-biotin/ds-DNA/STV complexes were formed with two free biotin sites on the STV (Fig. 8).[60] These complexes were successfully used in ultrasensitive detection of low molecular weight molecules via polymerase chain reaction (PCR) assays. Mirkin and co-workers have considered a three component system containing a biotinylated DNA single strand, STV, and gold nanoparticles functionalized with a complementary DNA single strand.[61] Macroscopic periodic architectures were observed in which the gold nanoparticles were aggregated through DNA/biotin/STV linkages. Moreover, the structures were reversibly disassembled by increasing the temperature above the DNA melting point.

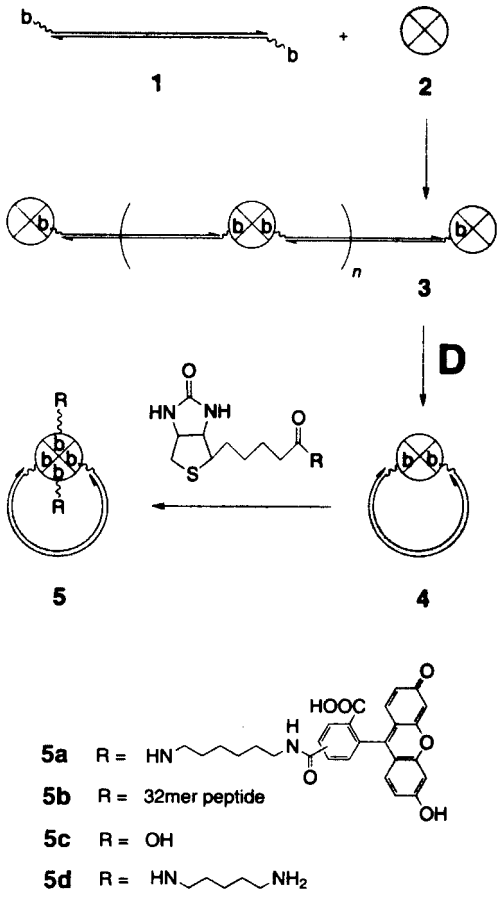

Fig. 8. Scheme showing synthesis of hapten (*R*)-functionalized DNA-STV nanocircles (**5**) from 5,5-bisbiotinylated (b) 169 base-pair ds-DNA oligonucleotide fragments (**1**) and STV (**2**). The oligomeric conjugates **3** are transformed into the nanocircles **4** by thermal treatment. The complementary DNA strands are drawn as parallel lines. The 3-ends are indicated by the arrow heads. Reproduced with permission from [60].

4.2.3. Nanoparticle-Based Programmed Assembly

This approach, which consists of attaching complementary oligonucleotides via covalent, electrostatic, or hydrogen bonding interactions to the surface of metallic or semi-conductor nanoparticles, is currently the focus of many research investigations. Particle self-assembly is then induced either in solution or at the surface of a solid substrate by duplex formation, which has the advantages of being highly selective and thermally reversible. Although it has been readily demonstrated that two complementary populations of DNA-capped nanoparticles spontaneously form large aggregates upon mixing, control over the geometry and the morphology of the superstructure remain a significant challenge. Parameters such as the number of oligonucleotides per particle,[62] nature of the solid surface,[8,63,64] and size and shape of the particles,[65] can have a major impact on the process of programmed assembly.

DNA pairing is a well-established recognition mechanism for encoding solid substrates. Recently, this approach has been extended to the fabrication of substrates with multiple

  0935-9648/02/1106-0783 $ 17.50+.50/0

Fig. 9. TEM image of large self-assembled aggregates of aligned gold nanorods formed by interparticle duplex linkages using surface-attached complementary 21-base pair oligonucleotides. Reproduced with permission from *Chemical Communications* [65]. Copyright 2001 Royal Society of Chemistry.

ordered arrays of gold particles by grafting two different oligonucleotides onto surface sites pre-defined with a scanning probe cantilever tip inked with a mercaptoacid.[8] Upon exposure of the surface to suspensions of gold particles covered with oligonucleotides complementary to one of the immobilized DNA strands, orthogonal self-assembly occurs, in which single particles of each of the two populations are pinned specifically to their corresponding sub-micrometer surface sites. In other work, multilayered arrays of DNA-functionalized cadmium sulfide (CdS) nanoparticles were organized layer by layer on a gold electrode surface using a set of two populations of DNA-capped CdS nanoparticles and a soluble free oligonucleotide half-complementary to each population.[63] By adding a ruthenium salt electrostatically immobilized along the DNA backbone, it was possible to generate photoelectrons by irradiation of the CdS nanoparticles, transfer the conduction electrons through the ruthenium complexes into the gold electrode and measure an enhanced photocurrent.

These examples are promising indications that DNA could play an important role as a self-assembling mortar and possible addressable code in materials with optical or electronic properties relevant to nanotechnologies.[66] However, most of the assembled materials are essentially isotropic or comprise randomly distributed features. In contrast, many aspects of functional nanostructures, such as optical, magnetic, and electronic properties, as well as device interconnection, depend on anisotropy either in the nanoscale building blocks or superstructural assembly. One possible approach to generate anisotropy and patterning is through the use of external fields; for example, directionality was achieved in the gold/DNA/CdS nanoparticle multilayers described above[63] by applying a voltage to the electrode. Alternatively, replacement of DNA-capped spherical nanoparticles with nanowires[64] or nanorods.[65] provides an internal bias for the anisotropic assembly of 2D and 3D arrays. In particular, gold nanowires, 200 nm in diameter and with aspect ratios of up to 30, were coated with thiolated oligonucleotides either on the entire surface or specifically at both tips. The wires were then tethered to DNA-functionalized glass surfaces and the 2D assemblies probed by standard fluorescent tags.[64] Three-dimensional aggregates of aligned gold nanorods have been produced by mixing two populations of nanorods derivatized with either two complementary thiolated oligonucleotides or two non-complementary strands in association with a soluble oligonucleotide with bipartite complementarity (Fig. 9).[65] Self-assembly occurs reversibly so that the superstructure, which consist of nanorods co-aligned side-by-side and interspaced by the DNA layer, can be disassembled by increasing the temperature of the solution above the chain melting temperature.

In this section, we have reviewed recent work on the use of self-assembly to build higher-order architectures. Materials based on DNA appear to offer much promise as supramolecular conjugates, templated nanostructures, and 3D ordered nanoparticle-based superstructures. In the latter case, the building blocks are traditional inorganic nanomaterials, but the cohesion forces maintaining the structural integrity are biomolecular in origin. This interplay between biological systems and nanochemistry is at the heart of the burgeoning area of bionanotechnology, which we discuss in the next section.

5. Bio-nanomaterials

The recent shift in emphasis towards materials science at the nanometer level continues to be strongly influenced and inspired by the study of small-scale biological structures and architectures. This size regime is common to both fields so that problems and discoveries in one discipline are very likely to be relevant to the other. Moreover, both research areas can be readily combined in the search for novel bio-nanomaterials with potential spin-offs in nanotechnology. This frontier, where nanosciences and biology meet, has been recently discussed in an excellent review by Niemeyer.[67] Here, we illustrate some of the latest results in this field.

5.1. Bio-inorganic Nanoparticles

One of the main areas of input involving biology and nanosciences is based on the biorecognition-induced assembly of inorganic nanoparticles, (see Sec. 4.2.3). Such systems offer much potential in bio-analytical chemistry. For example, biotinylated antibodies and streptavidin (STV)-functionalized oligonucleotides were used to cap DNA-covered gold nanoparticles with proteins.[68,69] The bio-nanocolloids were tested in sandwich immunoassays and revealed high stability, unal-

0935-9648/02/1106-0784 $ 17.50+.50/0

ADVANCED MATERIALS

tered specific recognition capabilities and a detection limit similar to standard immunoassays. A related approach involving block-by-block design with a bifunctional protein was used to specifically assemble dissimilar particles.[70] A gold-binding oligopeptide was sequenced and linked to a small biotin moiety for STV recognition. Assembly was observed when STV-functionalized polystyrene beads were mixed with gold particles in the presence of the biotinylated oligopeptide. In other work, bovine serum albumin (BSA) was conjugated to L-cysteine capped CdTe nanoparticles via a glutaric dialdehyde linker to produce mainly 1:1 BSA/CdTe conjugates.[71] These exhibited interesting optical cross-talk between the protein and nanoparticle surface, such that, whereas uncoupled BSA and CdTe fluoresce, the BSA and CdTe emissions were completely suppressed or more than doubled, respectively, in the bionanoparticle conjugate. Although a classical Förster energy transfer can explain the optical data, the observations remain unprecedented for a nanoparticle-based system.

The ability to organize bio-functionalized nanoparticles in 2D is an important requirement for device applications. Bio-inspired routes to surface patterning are often based on template-directed processes. For example, self-assembled 2D crystals of a bacterial surface layer protein (S-layer) were used to fabricate highly ordered superlattice arrays of gold nanoparticles by deposition from pre-formed colloids.[72] The S-layer template consisted of hexameric units arranged in a periodic (*p*6) hexagonal structure with lattice constant, 18 nm. Each hexamer was in the form of a hollow cone with a 2 nm wide positively charged central channel, and this site-specific surface periodicity was used to control the periodic assembly of negatively charged gold nanoparticles by electrostatic binding (Fig. 10). The interparticle center-to-center spacing (18 nm) was commensurate with the underlying S-layer template, and did not change when gold nanoparticles with diameters of 5 or 10 nm were used. However, the interparticle surface-to-surface spacings decreased with increasing particle size, suggesting that fine-tuning of the gap required for electronic tunneling between adjacent nanoparticles should be possible if appropriate gold colloids can be synthesized.

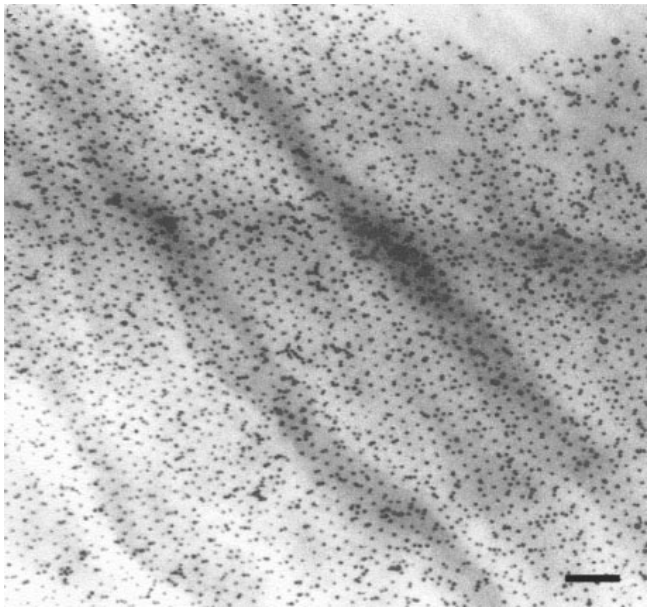

Fig. 10. TEM image showing S-layer templated periodic array of 5 nm sized gold nanoparticles. Scale bar is 100 nm. Reproduced with permission from [72].

The potential of biomolecular structures to sequester metal cations for materials synthesis has been highlighted in a number of studies. In particular, S-layers have been used to direct the synthesis of inorganic nanoparticles.[73] In this case, incubating the protein layers with metal salts, such as K_2PtCl_4 and K_2PdCl_4, followed by irradiation with an electron beam, produced a superlattice of 5 to 7 nm sized metallic nanoparticles at specific interstitial sites across the S-layer surface. One possibility is that the inner cavities of the protein layer serve as localized reservoirs of cations that are reduced in situ to metal clusters under the electron beam. Other studies have shown that the protein capsule of lumazine synthase can sequester Fe^{II} cations from solution and serve as a confined nanoscale environment for the synthesis of iron oxide nanoparticles.[74] Lumazine synthase is a hollow bacterial enzyme complex of 60 subunits with an inner cavity diameter of 7.8 nm surrounded by an icosahedral shell, 14.7 nm in outer diameter, and permeated by ten hydrophilic funnel-shaped channels. When incubated in the presence of a de-aerated aqueous solution of Fe^{II} ions, ion uptake followed by oxidation in air resulted in the specific nucleation and growth of crystalline lepidocrocite (γ-FeOOH) nanoparticles inside the capsid cavity. Alternatively, whole cells can be used as potential substrates for the biosynthesis of metallic nanoparticles by bioreduction of salts such as $[AuCl_4]^-$ and Ag^+. For example, upon exposure to these metal salt solutions, the fungus, *Verticilium sp.* produces 20 to 30 nm sized gold or silver nanoparticles on the mycelia wall surface or cytoplasmic membrane.[75,76] Although the mechanisms of metal incorporation and reduction were not established, it seems possible that specific enzymes or proteins within the cells were responsible for nanoparticle formation.

Bio-inspired routes to nanoparticle synthesis often involve the use of biomolecular capping agents or membrane-mimetic compartments such as vesicles and microemulsions. As an example of the first approach, histidine complexes of zinc or magnesium have been used to prepare Mn^{II}-doped ZnS nanocrystals.[77] The presence of histidine not only stabilized the 8 nm nanocrystals by surface capping, but also increased the solubility of ZnS to a level on par with MnS such that homogeneous levels of Mn^{II} doping in the ZnS structure were observed. In contrast, negligible doping occurred in pure aqueous solutions because of rapid precipitation due to the intrinsic low solubility of zinc sulfide. Moreover, when redispersed in aqueous media, the histidine-capped nanoparticles showed an orange fluorescence that should be useful in biolabeling applications. In the second approach, water-in-oil microemulsions have continued to be used extensively as confined reaction media for the synthesis of inorganic nanoparticles. Whereas most studies remain focused on classical inor-

  0935-9648/02/1106-0785 $ 17.50+.50/0

ganic materials such as oxides and sulfides, a recent report has developed this strategy for the synthesis of coordination compounds such as transition metal-based molecular magnets.[78] By combining two surfactant-stabilized microemulsions containing the individual reactants, discrete cubic or spherical nanoparticles of crystalline cobalt hexacyanoferrate, cobalt penta-cyanonitrosylferrate, or chromium hexacyanochromate were obtained (Fig. 11). Nucleation occurred by droplet collision to produce small clusters that subsequently aggregated into nanocubes or spheres with particle sizes determined by the surfactant/water molar ratio. Surface and size-dependent effects on the magnetic and magneto-optical properties of these nanomaterials are expected, and the demonstrated control over particle shape and size could be relevant to the implementation of molecule-based materials within functional devices.

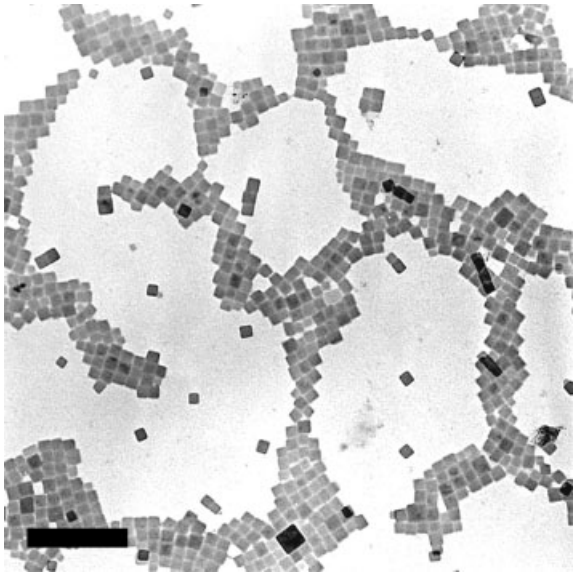

Fig. 11. TEM image showing 15 nm sized cobalt hexacyanoferrate nanocubes synthesized in water-in-oil microemulsions and partial superlattice assembly. Scale bar is 200 nm. Reproduced with permission from *Nano Letters* [78]. Copyright 2002 American Chemical Society.

5.2. Biotechnological Applications

Combinations of nanoparticles and biomolecules are expected to lead to new optical or magnetic tags for high-throughput screening applications in drug discovery and genomics. These biotechnological applications are based on the production of large chemical compound libraries, which are attached to a solid surface and rapidly screened for biological activity.[79,80] Due to limited substrate areas, current devices often display a restricted number of compounds ($< 10^5$), when libraries containing more than 10^6 may be required for high sensitivity. Moreover, the sequential nature of array fabrication and analysis often limits the efficiency of the approach and increases the cost. Recent attempts to circumvent these problems have focused on the use of colloidal silica particles to increase the total surface area of the substrate,[79] and as a means of applying a combinatorial "split and mix" method that is often employed for screening macromolecules synthesized from a limited number of monomers.[80]

In the first case, porous films were prepared by spin coating a colloidal suspension of 15 to 65 nm sized silica nanoparticles and then standard microarray probe immobilization techniques were applied to the porous substrate.[79] Chemical synthesis of the probe arrays was as efficient as on conventional flat glass substrates and increased amounts of the DNA targets were bound to the arrays because of penetration within the porous film. The hybridization signal, which reached 70 % of the surface area of the pores, was 20 times higher than flat glass for a 0.5 μm thick film. In the second example,[80] a colloidal silica suspension was divided into several batches, which were each functionalized with a specific monomer. After reaction, the batches were recombined, mixed, and re-divided before the next reaction step. After several cycles, the colloidal suspension consisted of a library of silica beads each of which comprised multiple copies of a specific sequence of monomers. By encoding the beads with a fluorescent barcode either before the first division or after each cycle, the extremely large library could be deciphered from the optical signature carried by the silica spheres.

A new detection technique combining magnetic iron oxide nanoparticles and oligonucleotides has been reported.[81] The approach was similar to that employed with oligonucleotide-coated gold nanoparticles, except that the reversibility between hybridization and denaturation states were monitored by spin–spin NMR relaxation time measurements (Fig. 12). Other studies have shown that double-stranded DNA when attached to gold nanoparticles can be locally addressed through inductive coupling.[82] In the presence of a radio-frequency magnetic field, local heating was induced at the surface of the gold nanoparticle such that the covalently linked DNA molecules were raised above the duplex melting temperature and denaturation was observed. Re-hybridization occurred as quickly as denaturation after the radio-frequency field was turned off because of fast thermalization. The re-

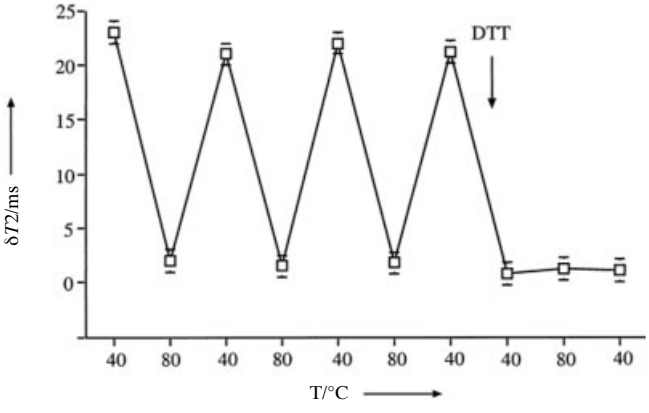

Fig. 12. Changes in the NMR T2 values of an aqueous solution containing iron oxide nanoparticles coated with complementary oligonucleotides as a function of temperature cycling. Reproduced with permission from [81].

0935-9648/02/1106-0786 $ 17.50+.50/0

ADVANCED MATERIALS

mote electrical control of DNA hybridization could have applications in actuators, DNA computation, or triggered messenger RNA production.

6. Conclusions

As described in this review, significant developments have been made in bio-inspired materials chemistry during the last year. The field continues to grow internationally and contribute to new interdisciplinary areas concerned with the synthesis, self-assembly, and processing of organized matter across a range of length scales. A wide range of soft, hard, or hybrid materials and interfaces are being explored with the promise of diverse applications in bioceramic implants, bio-nanotechnology, nanochemistry, and environmentally benign routes to functional materials. Bio-inspired materials are also of fundamental importance in biomedical engineering, for instance, in the design and fabrication of artificial muscles. For example, hinges made of electrochemically swollen or contracted polyaniline/pyrrole were combined with arms consisting of suspended metallic plates to produce a perpendicular actuator capable of lifting itself from the substrate and moving horizontally.[83] In the long term, the path from biological systems to bio-inspired materials could lead back to a new biology—*artificial biology*—in which the retro-fitting and adaptive evolution of biomimetic components become so commonplace that the physical nature of human life itself is transformed beyond our current imagination.

[1] S. Mann, *Biomineralization. Principles and Concepts in Bioinorganic Materials Chemistry*, Oxford University Press, Oxford, UK **2001**.
[2] S. Mann, *Biomimetic Materials Chemistry*, VCH, Weinheim **1996**.
[3] C. C. Dupont-Gillain, P. G. Rouxhet, *Nano Lett.* **2001**, *1*, 245.
[4] M. Niederweis, C. Heinz, K. Janik, S. H. Bossmann, *Nano Lett.* **2001**, *1*, 169.
[5] B. F. Erlanger, B.-X. Chen, M. Zhu, L. Brus, *Nano Lett.* **2001**, *1*, 465.
[6] S.-R. Kim, N. L. Abbott, *Adv. Mater.* **2001**, *13*, 1445.
[7] A. Loidl-Stahlhofen, J. Schmitt, J. Nöller, T. Hartmann, H. Brodowsky, W. Schmitt, J. Keldenich, *Adv. Mater.* **2001**, *13*, 1829.
[8] L. M. Demers, S.-J. Park, T. A. Taton, Z. Li, C. A. Mirkin, *Angew. Chem. Int. Ed.* **2001**, *40*, 3071.
[9] G. D. Bachand, R. K. Soong, H. P. Neves, A. Olkhovets, H. G. Craighead, C. D. Montemagno, *Nano Lett.* **2001**, *1*, 42.
[10] L. Limberis, J. J. Magda, R. J. Stewart, *Nano Lett.* **2001**, *1*, 277.
[11] H. Hess, J. Clemmens, D. Qin, J. Howard, V. Vogel, *Nano Lett.* **2001**, *1*, 235.
[12] H. Matsui, P. Porrata, G. E. Douberly, Jr., *Nano Lett.* **2001**, *1*, 461.
[13] A. Hengstenberg, A. Blöchl, I. D. Dietzel, W. Schuhmann, *Angew. Chem. Int. Ed.* **2001**, *40*, 905.
[14] C. Tromas, J. Rojo, J. M. de la Fuente, A. G. Barrientos, R. García, S. Penadés, *Angew. Chem. Int. Ed.* **2001**, *40*, 3052.
[15] S.-Y. Wu, J. Dornan, G. Kontopidis, P. Taylor, M. D. Walkinshaw, *Angew. Chem. Int. Ed.* **2001**, *40*, 582.
[16] M. Ueda, Y. Sako, T. Tanaka, P. Devreotes, T. Yanagida, *Science* **2001**, *293*, 864.
[17] I. Bontidean, A. Kumar, E. Csöregi, I. Yu. Galaev, B. Mattiasson, *Angew. Chem. Int. Ed.* **2001**, *40*, 2676.
[18] O. Hayden, F. L. Dickert, *Adv. Mater.* **2001**, *13*, 1480.
[19] H. Bayley, P. S. Cremer, *Nature* **2001**, *413*, 226.
[20] M. Ulbrich, P. Fromherz, *Adv. Mater.* **2001**, *13*, 344.
[21] J. O. Winter, T. Y. Liu, B. A. Korgel, C. E. Schmidt, *Adv. Mater.* **2001**, *13*, 1673.
[22] V. Chin, B. E. Collins, M. J. Sailor, S. N. Bhatia, *Adv. Mater.* **2001**, *13*, 1877.
[23] J. Aizenberg, A. Tkachenko, S. Weiner, L. Addadi, G. Hendler, *Nature* **2001**, *412*, 819.
[24] S. K. Lower, M. F. Hochella, Jr., T. J. Beveridge, *Science* **2001**, *293*, 1360.
[25] C. A. Orme, A. Noy, A. Wierzbicki, M. T. McBride, M. Grantham, H. H. Teng, P. M. Dove, J. J. DeYoreo, *Nature* **2001**, *411*, 775.
[26] K. Naka, Y. Chujo, *Chem. Mater.* **2001**, *13*, 3245.
[27] K. M. McGrath, *Adv. Mater.* **2001**, *13*, 989.
[28] N. Hosoda, T. Kato, *Chem. Mater.* **2001**, *13*, 688.
[29] I. Lee, S. W. Han, H. J. Choi, K. Kim, *Adv. Mater.* **2001**, *13*, 1617.
[30] S. Busch, U. Schwarz, R. Kniep, *Chem. Mater.* **2001**, *13*, 3260.
[31] A. Peytcheva, M. Antonietti, *Angew. Chem. Int. Ed.* **2001**, *40*, 3380.
[32] S. Murata, H. Furukawa, K. Kuroda, *Chem. Mater.* **2001**, *13*, 2722.
[33] S. Polarz, B. Smarsly, L. Bronstein, M. Antonietti, *Angew. Chem. Int. Ed.* **2001**, *40*, 4417.
[34] I. Gill, *Chem. Mater.* **2001**, *13*, 3404.
[35] A. Coiffier, T. Coradin, C. Roux, O. M. M. Bouvet, J. Livage, *J. Mater. Chem.* **2001**, *11*, 2039.
[36] J. R. Premkumar, O. Lev, R. Rosen, S. Belkin, *Adv. Mater.* **2001**, *13*, 1773.
[37] Y. Shin, J. Liu, J. H. Chang, Z. Nie, G. J. Exarhos, *Adv. Mater.* **2001**, *13*, 728.
[38] C. E. Fowler, W. Shenton, G. Stubbs, S. Mann, *Adv. Mater.* **2001**, *13*, 1266.
[39] Z. J. Shen, E. Adolfsson, M. Nygren, L. Gao, H. Kawaoka, K. Niihara, *Adv. Mater.* **2001**, *13*, 214.
[40] E. S. Ahn, N. J. Gleason, A. Nakahira, J. Y. Ying, *Nano Lett.* **2001**, *1*, 149.
[41] H. Takadama, H.-M. Kim, T. Kokubo, T. Nakamura, *Chem. Mater.* **2001**, *13*, 1108.
[42] a) T. Höche, C. Moisescu, I. Avramov, C. Rüssel, W. D. Heerdegen, C. Jäger, *Chem. Mater.* **2001**, *13*, 1312. b) T. Höche, C. Moisescu, I. Avramov, C. Rüssel, W. D. Heerdegen, C. Jäger, *Chem. Mater.* **2001**, *13*, 1320.
[43] H. Yan, K. Zhang, C. F. Blanford, L. F. Francis, A. Stein, *Chem. Mater.* **2001**, *13*, 1374.
[44] J. M. Gomez-Vega, A. Hozumi, H. Sugimura, O. Takai, *Adv. Mater.* **2001**, *13*, 822.
[45] J. D. Hartgerink, E. Beniash, S. I. Stupp, *Science* **2001**, *293*, 1684.
[46] M. Dubois, B. Demé, T. Gulik-Krzywicki, J.-C. Dedieu, C. Vautrin, S. Désert, E. Perez, T. Zemb, *Nature* **2001**, *411*, 672.
[47] M. S. Spector, A. Singh, P. B. Messersmith, J. M. Schnur, *Nano Lett.* **2001**, *1*, 375.
[48] D. T. Bong, M. R. Ghadiri, *Angew. Chem. Int. Ed.* **2001**, *40*, 2163.
[49] D. Gauthier, P. Baillargeon, M. Drouin, Y. L. Dory, *Angew. Chem. Int. Ed.* **2001**, *40*, 4635.
[50] D. T. Bong, T. D. Clark, J. R. Granja, M. R. Ghadiri, *Angew. Chem. Int. Ed.* **2001**, *40*, 988.
[51] G. Das, L. Ouali, M. Adrian, B. Baumeister, K. J. Wilkinson, S. Matile, *Angew. Chem. Int. Ed.* **2001**, *40*, 4657.
[52] T. Surrey, F. Nédélec, S. Leibler, E. Karsenti, *Science* **2001**, *293*, 1167.
[53] L. Wang, J. Yoshida, N. Ogata, S. Sasaki, T. Kajiyama, *Chem. Mater.* **2001**, *13*, 1273.
[54] S. Uemura, T. Shimakawa, K. Kusabuka, T. Nakahira, N. Kobayashi, *J. Mater. Chem.* **2001**, *11*, 267.
[55] N. Kobayashi, S. Uemura, K. Kusabuka, T. Nakahira, H. Takahashi, *J. Mater. Chem.* **2001**, *11*, 1766.
[56] I. Vargas-Baca, D. Mitra, H. J. Zulyniak, J. Banerjee, H. F. Sleiman, *Angew. Chem. Int. Ed.* **2001**, *40*, 4629.
[57] M. J. Hannon, V. Moreno, M. J. Prieto, E. Moldrheim, E: Sletten, I. Meistermann, C. J. Isaac, K. J. Sanders, A. Rodger, *Angew. Chem. Int. Ed.* **2001**, *40*, 879.
[58] W. E. Ford, O. Harnack, A. Yasuda, J. M. Wessels, *Adv. Mater.* **2001**, *13*, 1793.
[59] A. Kumar, M. Pattarkine, M. Bhadbhade, A. B. Mandale, K. N. Ganesh, S. S. Datar, C. V. Dharmadhikari, M. Sastry, *Adv. Mater.* **2001**, *13*, 341.
[60] C. M. Niemeyer, R. Wacker, M. Adler, *Angew. Chem. Int. Ed.* **2001**, *40*, 3169.
[61] S.-J. Park, A. A. Lazarides, C. A. Mirkin, R. L. Letsinger, *Angew. Chem. Int. Ed.* **2001**, *40*, 2909.
[62] D. Zanchet, C. M. Micheel, W. J. Parak, D. Gerion, A. P. Alivisatos, *Nano Lett.* **2001**, *1*, 32.
[63] I. Willner, F. Patolsky, J. Wasserman, *Angew. Chem. Int. Ed.* **2001**, *40*, 1861.
[64] J. K. N. Mbindyo, B. D. Reiss, B. R. Martin, C. D. Keating, M. J. Natan, T. E. Mallouk, *Adv. Mater.* **2001**, *13*, 249.
[65] E. Dujardin, L.-B. Hsin, C. R. C. Wang, S. Mann, *Chem. Commun.* **2001**, 1264.
[66] N. C. Seeman, *Nano Lett.* **2001**, *1*, 22.
[67] C. M. Niemeyer, *Angew. Chem. Int. Ed.* **2001**, *40*, 4128.

  0935-9648/02/1106-0787 $ 17.50+.50/0

[68] C. M. Niemeyer, B. Ceyhan, *Angew. Chem. Int. Ed.* **2001**, *40*, 3685.
[69] C. M. Niemeyer, B. Ceyhan, *Angew. Chem. Int. Ed.* **2001**, *40*, 3798.
[70] S. Brown, *Nano Lett.* **2001**, *1*, 391.
[71] N. N. Mamedova, N. A. Kotov, A. L. Rogach, J. Studer, *Nano Lett.* **2001**, *1*, 281.
[72] S. R. Hall, W. Shenton, H. Engelhardt, S. Mann, *ChemPhysChem* **2001**, *2*, 184.
[73] R. Wahl, M. Mertig, J. Raff, S. Selenska-Pobell, W. Pompe, *Adv. Mater.* **2001**, *13*, 736.
[74] W. Shenton, S. Mann, H. Cölfen, A. Bacher, M. Fischer, *Angew. Chem. Int. Ed.* **2001**, *40*, 442.
[75] P. Mukherjee, A. Ahmad, D. Mandal, S. Senapati, S. R. Sainkar, M. I. Khan, R. Parishcha, P. V. Ajaykumar, M. Alam, R. Kumar, M. Sastry, *Nano Lett.* **2001**, *1*, 515.
[76] P. Mukherjee, A. Ahmad, D. Mandal, S. Senapati, S. R. Sainkar, M. I. Khan, R. Ramani, R. Parischa, P. V. Ajayakumar, M. Alam, M. Sastry, R. Kumar, *Angew. Chem. Int. Ed.* **2001**, *40*, 3585.
[77] G. Yi, B. Sun, F. Yang, D. Chen, *J. Mater. Chem.* **2001**, *11*, 2928.
[78] S. Vaucher, J. Fielden, M. Li, E. Dujardin, S. Mann, *Nano Lett.* **2002**, *2*, 225.
[79] M. Glazer, J. Fidanza, G. McGall, C. Frank, *Chem. Mater.* **2001**, *13*, 4773.
[80] M. Trau, B. J. Battersby, *Adv. Mater.* **2001**, *13*, 975.
[81] L. Josephson, J. M. Perez, R. Weissleder, *Angew. Chem. Int. Ed.* **2001**, *40*, 3204.
[82] K. Hamad-Schifferli, J. J. Schwartz, A. T. Santos, S. Zhang, J. M. Jacobson, *Nature* **2001**, *415*, 152.
[83] E. W. H. Jager, O. Inganäs, I. Lundström, *Adv. Mater.* **2001**, *13*, 76.

  0935-9648/02/1106-0788 $ 17.50+.50/0